ISSN 1070-3632, Russian Journal of General Chemistry, 2016, Vol. 86, No. 5, pp. 1054–1063. © Pleiades Publishing, Ltd., 2016.
Original Russian Text © I.E. Mikhailov, N.I. Vikrishchuk, L.D. Popov, G.A. Dushenko, A.D. Beldovskaya, Yu.V. Revinskii, V.I. Minkin, 2016, published in Zhurnal Obshchei Khimii, 2016, Vol. 86, No. 5, pp. 791–801.

Absorption and Luminescence Spectra of 5-Aryl-3-methyl-1,2,4-oxadiazoles and Their Chelate Complexes with Zinc(II) and Copper(II)

I. E. Mikhailov[a,b], N. I. Vikrishchuk[c], L. D. Popov[c], G. A. Dushenko[a,b], A. D. Beldovskaya[d], Yu. V. Revinskii[a], and V. I. Minkin[b]

[a] *Southern Scientific Center, Russian Academy of Sciences, ul. Chekhova 41, Rostov-on-Don, 344006 Russia e-mail: mikhail@ipoc.rsu.ru*

[b] *Research Institute of Physical and Organic Chemistry, Southern Federal University, pr. Stachki 194/2, Rostov-on-Don, 344090 Russia*

[c] *Southern Federal University, Bol'shaya Sadovaya ul. 105/42, Rostov-on-Don, 344006 Russia*

[d] *Institute of Arid Zones, Southern Scientific Center, Russian Academy of Sciences, ul. Chekhova 41, Rostov-on-Don, 344006 Russia*

Received August 27, 2015

Abstract—5-(2-Hydroxyphenyl)-3-methyl-1,2,4-oxadiazole and its *O*-methyl and *O*-acyl derivatives, as well as zinc(II) and copper(II) chelates, were synthesized. All these compounds showed luminescence with the emission maxima ranging from λ = 332 to 490 nm, but only 5-(2-methoxyphenyl)- and 5-(2-acetoxyphenyl)-3-methyl-1,2,4-oxadiazoles and zinc(II) complex of 5-(2-hydroxyphenyl)-3-methyl-1,2,4-oxadiazole were characterized by high luminescence quantum yield (φ = 0.308–0.452, 0.089–0.153, and 0.115–0.334, respectively). Stable conformers of 5-(2-hydroxyphenyl)-3-methyl-1,2,4-oxadiazole with different structures of the coordination entity were identified by DFT quantum chemical calculations.

Keywords: 5-aryl-3-methyl-1,2,4-oxadiazoles, electronic absorption and luminescence spectra, luminescence quantum yield, quantum chemical calculations

DOI: 10.1134/S1070363216050121

Bidentate heterocyclic ligands with an =N-(O_{phenol}) chelating moiety are widely used in the preparation of highly efficient organic [1, 2] and metal complex luminophores [3] and electron transport materials for organic light-emitting diodes (OLEDs) [4, 5]. Among such compounds, of particular interest are *o*-hydroxyphenyloxadiazoles and their derivatives, which additionally exhibit high biological activity and structural variability and are synthetically accessible. Although luminescence properties of 1,3,4-oxadiazoles and their dependence on structural factors have been well documented [5], analogous information for isomeric 1,2,4-oxadiazoles is rather poor. It has been reported that 1,2,4-oxadiazoles usually show luminescence in the visible region with low quantum yields [6]. Taking the above stated into account, the goal of the present work was to study the effect of structural factors on the luminescence properties of both previously known and newly synthesized 1,2,4-oxadiazoles with a view to revealing highly efficient organic and metal complex luminophores in this series of compounds.

5-(2-Hydroxyphenyl)-3-methyl-1,2,4-oxadiazole (**2**) was synthesized by recyclization of 2-methyl-4-oxo-1,3-benzoxazinium perchlorate (**1**) [7] with hydroxylamine, and alkylation of **2** with dimethyl sulfate in the presence of sodium hydroxide gave methyl ether **3a**. Treatment of **2** with acetic anhydride in the presence of a catalytic amount of 70% perchloric acid afforded acetate **3b**, and the reactions of **2** with benzoyl chloride in pyridine and with *p*-toluenesulfonyl chloride in ethyl methyl ketone in the presence of anhydrous potassium carbonate led to benzoate **3c** and *p*-toluenesulfonate **3d**, respectively. Zinc(II) and copper(II) chelates **4a** and **4b** with the composition ML_2 were synthesized by heating oxadiazole **2** with 0.5 equiv of

Scheme 1.

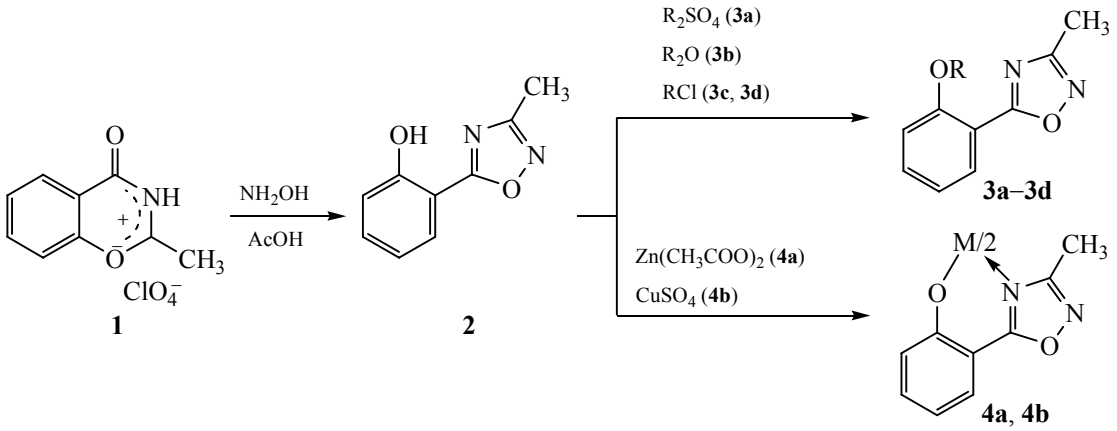

3, R = Me (**a**), Ac (**b**), Bz (**c**), Ts (**d**); **4**, M = Zn (**a**), Cu (**b**).

zinc(II) acetate or copper(II) sulfate, respectively, in boiling methanol (Scheme 1).

The structure of the synthesized compounds was determined on the basis of their elemental analyses and IR, ^{1}H and ^{13}C NMR, and mass spectra. Compounds **2**, **3a**–**3d**, **4a**, and **4b** were studied by electronic spectroscopy and fluorescence analysis. Quantum chemical calculations revealed stable conformers of **2** with different structures of the coordination entities.

The IR spectrum of **2** contained a broadened absorption band at 3179 cm^{-1} due to stretching vibrations of the phenolic hydroxy group involved in intramolecular hydrogen bond with the N^4 atom of the oxadiazole ring. No such band was observed in the spectra of **3** and **4** due to replacement of the hydroxy proton by alkyl or acyl group or metal ion; instead, strong absorption bands belonging to the corresponding functional group appeared (**3b**, 1756 cm^{-1}, C=O; **3c**, 1732 cm^{-1}, C=O; **3d**, 1171, 1374 cm^{-1}, SO_2). The complexation of **2** with metal ions was accompanied by low-frequency shift of the $C^5{=}N^4$ (1572, 1573 cm^{-1}; $\Delta\nu$ 10–18 cm^{-1}) and $C^3{-}N^4$ stretching bands (1471, 1477 cm^{-1}; $\Delta\nu$ 8–24 cm^{-1}) relative to the respective bands in the spectra of **2** and **3a**–**3d**; the shift of the $C^3{=}N^2$ stretching band (1606–1616 cm^{-1}) was smaller ($\Delta\nu$ 4–10 cm^{-1}) since that bond was not directly involved in the complexation. Analogous considerable decrease of the $C^3{-}N^4$ stretching vibration frequency of a structural analog of **4b**, bis[2-(3-phenyl-1,2,4-oxadiazol-5-yl)phenolato]copper(II), by 21 cm^{-1} compared to the free ligand, was reported in [8].

In the ^{1}H NMR spectra of **2**, **3a**–**3d** ($CDCl_3$), and **4a** (DMSO-d_6), protons of the methyl group in the oxadiazole ring gave a signal at δ 2.31–2.63 ppm, and aromatic protons resonated in the region 6.09–8.29 ppm. The spectra of **2**, **3a**, **3b**, and **3d** also contained signals of hydroxy (**2**), methoxy (**3a**), acetyl (**3b**), and tosyl methyl protons (**3d**) at δ 10.47, 3.92, 2.47, and 2.40 ppm, respectively. The ^{13}C NMR spectra of **2** and **3a**–**3d** displayed signals of all structural fragments of their molecules. The ^{13}C signals were assigned by analysis of long-range $^{13}C{-}^1H$ coupling constants for quaternary carbon atoms and the corresponding chemical shifts. For example, the C^3 signal appeared as a quartet due to long-range coupling with protons of the 3-CH_3 group [δ_C 173.80 ppm, $^2J_{CH}$ = 7.5 Hz (**2**); 167.64 ppm, $^2J_{CH}$ = 7.6 Hz (**3a**); 167.93 ppm, $^2J_{CH}$ = 7.6 Hz (**3b**); 167.85 ppm, $^2J_{CH}$ = 7.6 Hz (**3c**); 167.69 ppm, $^2J_{CH}$ = 7.6 Hz (**3d**)]. The C^5 signal was a doublet due to long-range coupling with the 6′-H proton in the phenol ring [δ_C 168.31 ppm, $^3J_{CH}$ = 3.2 Hz (**2**); 174.88 ppm, $^3J_{CH}$ = 4.4 Hz (**3a**); 173.18 ppm, $^3J_{CH}$ = 4.2 Hz (**3b**); 173.38 ppm, $^3J_{CH}$ = 4.4 Hz (**3c**), 172.99 ppm, $^2J_{CH}$ = 4.4 Hz (**3d**)]. The $C^{2'}$ atom in the phenol fragment showed couplings with 3′-H and 4′-H, so that its signal was a doublet of doublets [δ_C 161.26 ppm, $^2J_{CH}$ = 5.8 Hz, $^3J_{CH}$ = 5.6 Hz (**2**); 158.74 ppm, $^2J_{CH}$ = 6.9 Hz, $^3J_{CH}$ = 6.7 Hz (**3a**); 149.64 ppm, $^2J_{CH}$ = 7.9 Hz, $^3J_{CH}$ = 7.7 Hz (**3b**); 149.90 ppm, $^2J_{CH}$ = 6.5 Hz, $^3J_{CH}$ = 6.4 Hz (**3c**); 147.59 ppm, $^2J_{CH}$ = 7.5 Hz, $^3J_{CH}$ = 7.3 Hz (**3d**)]. The $C^{1'}$ nucleus resonated in a stronger field than the other quaternary carbons (due to the presence of phenolic oxygen atom in the neighboring position), and its signal had the same multiplicity due to long-range couplings with 5′-H and 6′-H [δ_C 114.10 ppm, $^2J_{CH}$ = 4.4 Hz, $^3J_{CH}$ = 4.3 Hz (**2**); 113.78 ppm, $^2J_{CH}$ = 4.4 Hz, $^3J_{CH}$ = 4.3 Hz (**3a**); 118.25 ppm, $^2J_{CH}$ = 5.2 Hz,

Scheme 2.

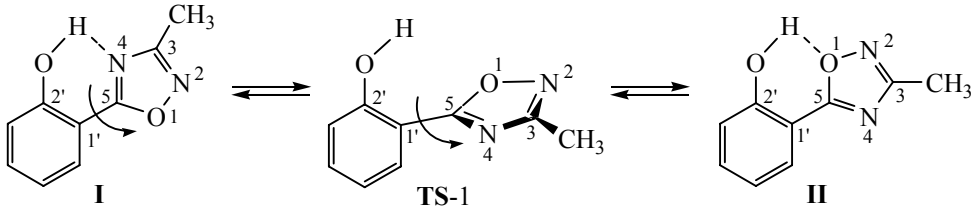

Scheme 3.

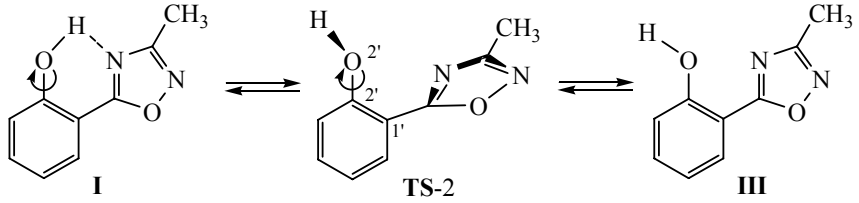

$^3J_{CH}$ = 5.1 Hz (**3b**); 118.43 ppm, $^2J_{CH}$ = 5.3 Hz, $^3J_{CH}$ = 5.2 Hz (**3c**); 119.29 ppm, $^2J_{CH}$ = 5.8 Hz, $^3J_{CH}$ = 5.7 Hz (**3d**)]. The other quaternary carbon signals were observed in the proton-coupled ^{13}C NMR spectra at δ_C 170.09 [q, $^2J_{CH}$ = 6.9 Hz, C=O (**3b**)], 129.88 [t, $^2J_{CH}$ = 5.3 Hz, C_6H_5 (**3c**)], 165.72 [t, $^3J_{CH}$ = 4.5 Hz, C=O (**3c**)], 132.36 [t, $^2J_{CH}$ = 8.8 Hz, C–SO_2 (**3d**)], and 146.07 [q, $^2J_{CH}$ = 6.9 Hz, **C**–CH_3 (**3d**)]. This spectral pattern was consistent with the ^{13}C NMR spectra of structurally similar triazoles [9, 10].

The mass spectra of oxadiazoles **2** and **3** and metal complexes **4** contained the molecular ion peaks whose fragmentation involved mainly synchronous cleavage of the N^4–C^3 and C^5–O bonds, as well as N^4–C^5 and N^2–O bonds, of the oxadiazole ring with formation of $[ArC{\equiv}NH]^+$ and $[ArC{\equiv}O]^+$ fragment ions. Subsequent decomposition of the latter produced low-molecular-weight ions. The low intensity (5–15%) of the molecular ions of *O*-acyl derivatives **3c** and **3d** is related to their instability. These molecular ions readily decompose into the initial oxadiazole fragment and acyl group whose intense peaks are observed in the mass spectra. Apart from the molecular ion peaks, complexes **4a** and **4b** showed in the mass spectra fragment ions resulting from elimination of one ligand and those corresponding to fragmentation of the ligand.

Molecules of oxadiazoles **2** and **3** are conformationally nonrigid due to free rotation of the phenol and oxadiazole fragments about the C–C single bond connecting them. This rotation could give rise to metal complexes with structurally different coordination entities. Therefore, we performed a theoretical study of the electronic and steric structure and relative stabilities of conformers of 5-(2-hydroxyphenyl)-3-methyl-1,2,4-oxadiazole (**2**) with different chelating moieties in terms of the density functional theory (DFT) and calculated energy barriers for rotation about the single bond connecting the hydroxyphenyl and oxadiazole rings, as well as about the C–OH bond (Scheme 2).

As a result, structures **I**–**IV** were localized as minima on the potential energy surface (PES) of 5-(2-hydroxyphenyl)-3-methyl-1,2,4-oxadiazole (**2**) (Fig. 1, Table 1). Rotamers **I** and **II** resulting from rotation about the $C^{1'}$–C^5 bond are characterized by fairly similar energies (ΔE_{ZPE} = 4.1 kcal/mol), and structure **I** corresponds to the global minimum on the PES. The energy barrier to the transformation **I**→**II** through transition state **TS**-1 is 12.0 kcal/mol (Fig. 2, Table 1). The benzene and oxadiazole rings in **TS**-1 are almost orthogonal to each other (torsion angle $C^{2'}C^{1'}C^5N^4$ 94.3°). The calculations predict the existence of both these rotamers which are rapidly interconverted via rotation about the $C^{1'}$–C^5 bond. In fact, in the ^{1}H and ^{13}C NMR spectra of **2** at room temperature we observed a set of signals assignable to an averaged structure, and the downfield shift of the OH signal in the ^{1}H NMR spectrum (δ 10.47 ppm) indicates strong intramolecular hydrogen bond between the OH proton and N^4 or oxygen atom of the oxadiazole ring.

Rotamer **III** with *exo* orientation of the hydroxy group (rotation about the C–OH bond) is less stable than **I** by 10.0 kcal/mol, so that the probability of its formation is very low. The energy barrier to the transformation **I** → **III** through transition state **TS**-2 is 12.3 kcal/mol (Fig. 2, Table 1, Scheme 3). The

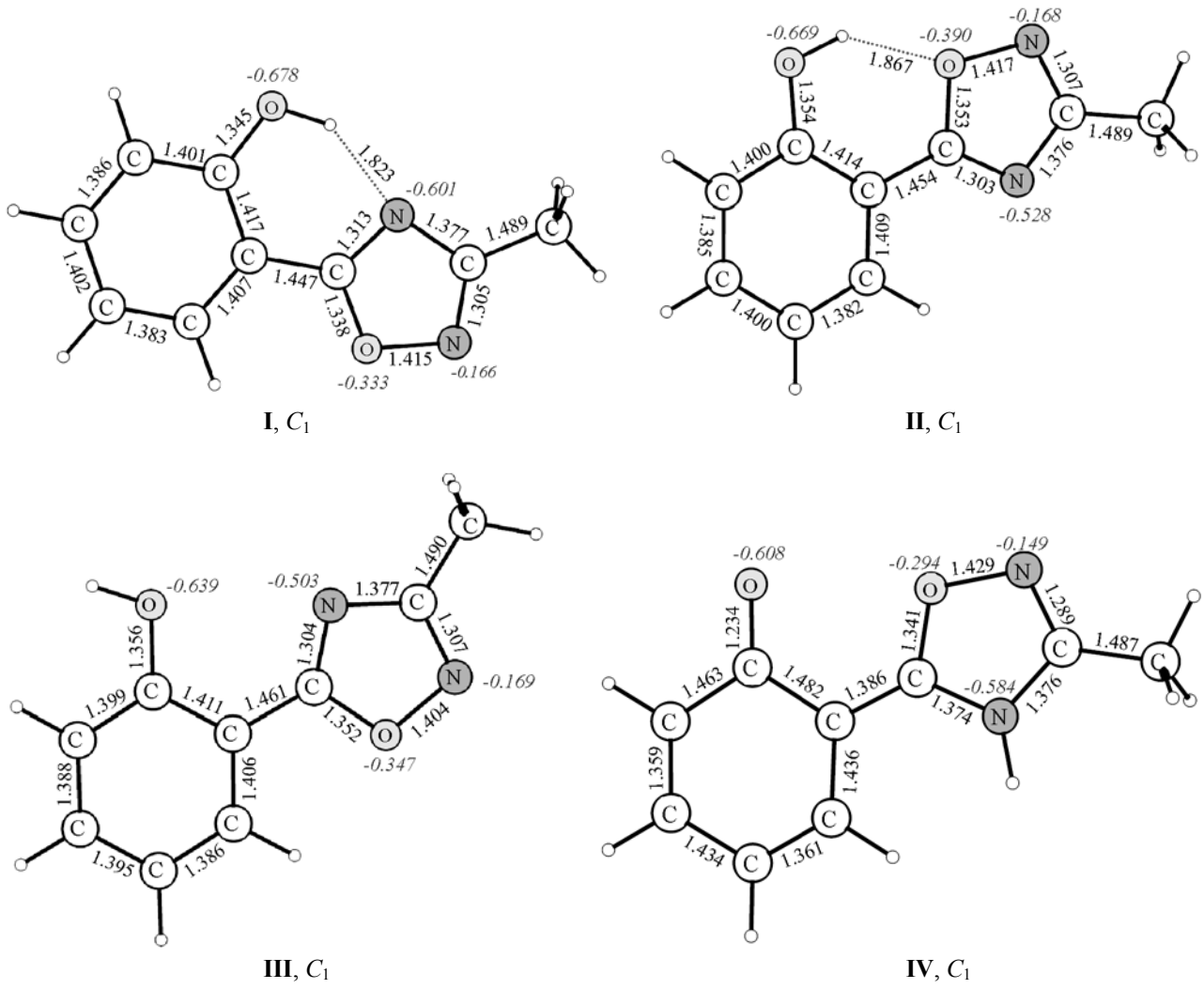

I, C_1 **II**, C_1

III, C_1 **IV**, C_1

Fig. 1. Calculated [B3LYP/6-311++G(*d*,*p*)] geometric parameters and charges on atoms (italicized numbers) of structures **I**–**IV** in the ground state (gas phase). Hereinafter, bond lengths are given in Å.

hydroxy group in **TS**-2 is forced out from the benzene ring plane so that the torsion angle $C^{1'}C^{2'}O^{2'}H$ is –113.3°. The large difference in the thermodynamic stabilities of structures **I** and **III** may be rationalized by stabilization of the former by intramolecular hydrogen bond (Fig. 1). This hydrogen bond is also responsible for the high energy barrier to the rotation about the C–OH bond which is not typical of such processes.

Intramolecular hydrogen bond between the OH proton and nitrogen atom of the oxadiazole ring should favor hydrogen transfer with formation of quinoid tautomer **V** (Scheme 4). However, structure **V** turned out to be unstable, and it was not localized on the PES of **2**. The ketone structure was identified as local minimum **IV** with the oxadiazole fragment turned through an angle of 180° with respect to **V**. Isomer **IV** is less stable than rotamer **I** by 33.0 kcal/mol (Table 1); therefore, proton transfer in the ground state is impossible.

However, the formation of quinoid isomer **V** is possible via excited-state intramolecular proton transfer (ESIPT) from the phenolic OH group on the oxa-

Scheme 4.

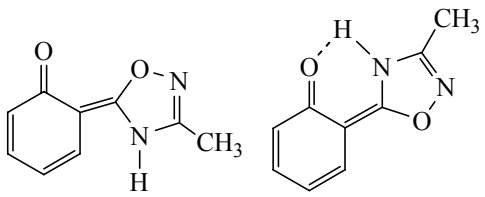

IV **V**

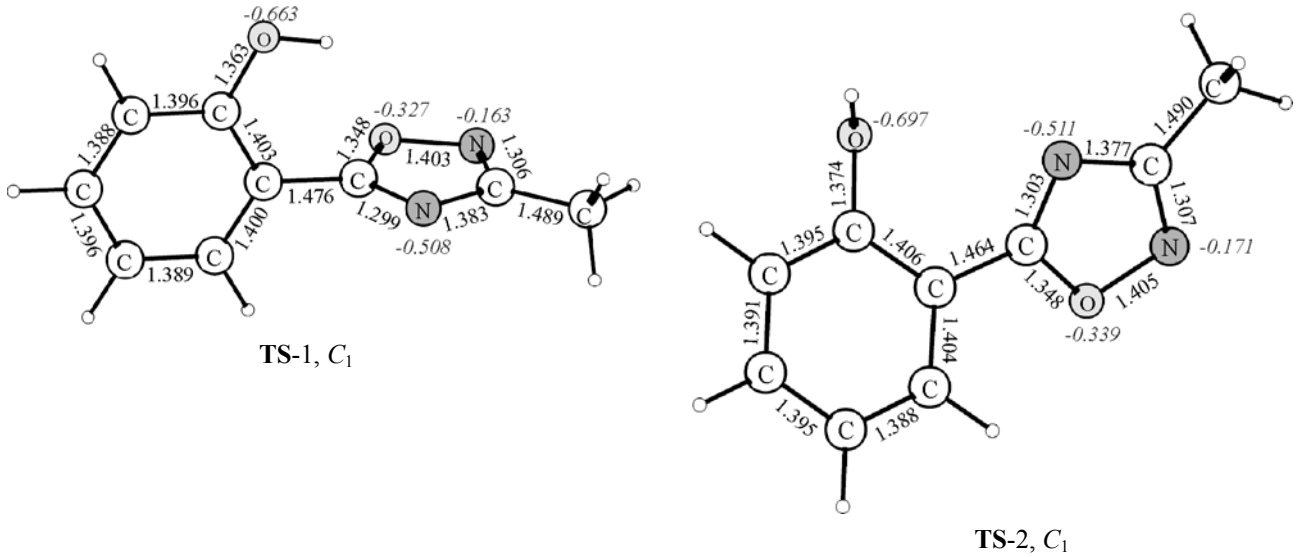

TS-1, C_1 **TS**-2, C_1

Fig. 2. Calculated [B3LYP/6-311++G(*d*,*p*)] geometric parameters and charges on atoms of transition states **TS**-1 and **TS**-2.

diazole nitrogen atom, which is facilitated by considerable increase of the acidity of the phenolic hydroxy group and basicity of the imino nitrogen atom in going to the excited state. Excited-state intramolecular proton transfer was observed for structurally related 2-(2-hydroxyphenyl)-5-aryl-1,3,4-oxadiazoles [11].

In the electronic absorption spectra of oxadiazoles **2** and **3** in both polar (DMSO, acetonitrile, methanol) and nonpolar solvents (isooctane, toluene), the long-wave absorption maximum arising from π–π* transitions is located in the λ range 248–315 nm (Table 2), which is typical of benzoid structure **I**. There is no distinct relation between the position of the long-wave absorption maximum and solvent polarity; however, an appreciable blue shift is observed as the acceptor power of the substituent on the phenolic oxygen atom increases. For instance, the blue shift is as large as 52–67 nm in all solvents in going from compound **2** to tosyloxy derivative **3d**. Analogous shift for *O*-acetyl and *O*-benzoyl derivatives **3b** and **3c** is smaller (Δλ = 13–56 nm), and the long-wave absorption maximum of **3c** appears at shorter wavelength than that of **3b**, in keeping with the acceptor power of the O-substituent (Table 2).

Table 1. Total and relative energies of conformers and tautomers of compound **2** in the ground state and transition states for their mutual transformations in the gas phase, calculated by the B3LYP/6-311++G(*d*,*p*) method[a]

Structure	E_{tot}, a.u.	ΔE_{ZPE}, kcal/mol	ω_1, cm^{-1}
I	–607.87467	0[b]	69
TS-1	–607.85437	12.0	–79[c]
II	–607.86771	4.1	49
TS-2	–607.85326	12.3	–409[c]
III	–607.85771	10.0	18
IV	–607.82011	33.0	48

[a] E_{tot} is the total energy, 1 a. u. = 627.5095 kcal/mol; ΔE_{ZPE} is the relative energy corrected for zero-point harmonic vibration energy; ω_1, cm^{-1} is the least harmonic vibration frequency.
[b] E_{ZPE} = –607.71516 a. u. for compound **2**.
[c] The single imaginary harmonic vibration frequency.

Even greater differences were observed in the luminescence spectra of compounds **2** and **3**. Oxadiazole **2** showed in the luminescence spectrum two bands with their maxima at λ 341–361 and 440–490 nm (Table 2). The short-wave band may be assigned to emission of the initial benzoid structure **I**, and the long-wave band, to photoinduced tautomer **V** generated by ESIPT from the phenolic hydroxy group to the nearest nitrogen atom of the heterocycle. As followed from the corresponding luminescence excitation spectra, oxadiazole **2** in the ground state is represented by two rotamers **I** and **II** existing in a dynamic equilibrium. Excitation of rotamer **II** gives rise to luminescence with a normal Stokes shift (2616–4453 cm^{-1}), whereas excited-state intramolecular proton transfer in rotamer **I** leads to photoinduced tautomer **V** which shows luminescence with an

Table 2. Electronic absorption and fluorescence spectra (λ_{excit} = 250–360 nm) of compounds **2**–**4**

Comp. no.	λ_{max}, nm ($\varepsilon \times 10^{-4}$, L mol^{-1} cm^{-1})			λ^{fl}_{max}, nm (φ)		
	toluene	acetonitrile	DMSO	toluene	acetonitrile	DMSO
2	315 (0.623)	255 (1.543)	311 (0.892)	350, 482	355, 476	361, 440
		312 (0.637)		(0.008[a])	(0.019[a])	(0.031[a])
	256[b] (0.770)	248[c] (1.564)		341, 490[b]	360, 450[c]	
	313 (0.333)	311 (0.604)		(0.007[a])	(0.015[a])	
3a	304 (0.619)	251 (1.242)	306 (0.589)	344	353	356
		303 (0.587)		(0.452)	(0.387)	(0.308)
		252[c] (1.410)			357[c]	
		304 (0.660)			(0.429)	
3b	295 (1.603)	249 (1.555)	290 (0.327)	337	332	339
		280 (0.277)		(0.095)	(0.153)	(0.089)
3c	285 (1.231)	234 (0.968)	290 (0.945)	340	351	360
		260 (0.527)		(0.003)	(0.001)	(0.002)
		234[c] (0.833)			337[c]	
		259 (0.474)			(0.002)	
3d[d]	227[b] (2.174)	230 (2.179)		345[b]	349	
	248 (1.143)	251 (1.216)		(0.001)	(0.002)	
		230[c] (2.674)			346[c]	
		250 (1.475)			(0.001)	
4a[e]		316 (2.125)	364 (1.75)		427	429
		362 (1.644)			(0.115)	(0.334)
4b[e]		300 (0.882)	366		421	430
		361 (1.548)	(1.623)		(0.001)	(0.001)

[a] Overall quantum yield.
[b] In isooctane.
[c] In methanol.
[d] Toluene and DMSO were not used since these solvents obscured the absorption of **3d**.
[e] Complexes **4a** and **4b** are insoluble in toluene.

anomalously large Stokes shift (9427–11541 cm^{-1}). Strong intramolecular hydrogen bond between the phenolic hydroxy proton and N^4 in **I** favors photoinduced proton transfer with formation of excited quinoid structure **V**. The existence of rotamers **I** and **II** in the ground state is also confirmed by the dependence of the emission intensity of **2** upon excitation wavelength. Unlike electronic absorption spectra, solvent polarity essentially affects the position of luminescence maxima and their intensity in the emission spectra of **2** (Table 2). In polar solvents, the short-wave emission maximum shifts red by 5–20 nm and the long-wave maximum shifts blue by 6–50 nm relative to their positions in nonpolar solvents (Table 2). Furthermore, the long-wave emission band of **2** in nonpolar solvents is more intense (by a factor of 1.6–2.5) than the short-wave maximum, while the opposite pattern is observed in polar solvents. The low luminescence quantum yield of **2** may be accounted for by nonradiative deactivation of the excited state according to the ESIPT mechanism [11] through rotamer **I**; insofar as the latter predominates in nonpolar medium due to stabilization by intramolecular hydrogen bond, the overall quantum yield in polar solvents is somewhat higher [φ = 0.015 (methanol), 0.019 (acetonitrile), 0.031 (DMSO)] than in nonpolar medium [φ = 0.007 (isooctane), 0.008 (toluene)]. Analogous pattern was observed previously for structurally related 5-aryl-2-(2-hydroxyphenyl)-1,3,4-oxadiazoles [11, 12] and 5-aryl-2-(2-hydroxyphenyl)-1,3,4-triazoles [10, 13].

Unlike oxadiazole **2**, methoxy derivative **3a** showed intense luminescence with a quantum yield φ of 0.308–0.452, and its luminescence spectrum contained only one short-wave emission maximum at λ = 440–490 nm

(Table 2). The lack of acidic hydroxy proton in molecule **3a** makes ESIPT process leading to quinoid structure impossible, so that the only short-wave emission band should be assigned to the benzoid structure. This is also confirmed by the position of the luminescence maximum of **3a**, which (as with compound **2**) shifts red in going to polar solvents, and by the luminescence excitation spectra. Analogous spectral behavior was found for 2-styrylquinolines in which the labile 8-OH proton was replaced by methyl or benzyl group [14, 15]; as a result, highly efficient luminophores emitting in the short-wave part of the visible region were obtained.

Likewise, no ESIPT is possible for oxadiazoles **3b**–**3d**, and only one short-wave maximum was present in their luminescence spectra (λ_{max}^{fl} = 332–360 nm; Table 2). The luminescence quantum yield of acetoxy derivative **3b** (φ = 0.089–0.153) is considerably higher than those of **3c** and **3d** (φ = 0.001–0.003). The low luminescence quantum yields of **3c** and **3d** may be rationalized by the lower energy of singlet and triplet *n*–π* states arising from the presence of heteroatoms in the substituents on the phenolic oxygen atom, in comparison to the corresponding π–π* states. The same also applies to 5-aryl-2-(2-benzoyloxyphenyl)-1,3,4-oxadiazoles [16, 17], quinolin-8-yl benzoates [18], and 2-styrylquinolin-8-yl *p*-toluenesulfonates [15]. Increased probability of singlet–triplet intersystem crossing between the π–π* and *n*–π* levels of non-conjugated oxadiazole and benzoyl (toluenesulfonyl) fragments favors nonradiative deactivation of the excited state [19], which reduces the luminescence quantum yield of **3c** and **3d** as compared to oxadiazole **3b** with higher energy of the *n*–π* levels of the acetyl fragment [20].

Although metal complexes **4a** and **4b** absorb at longer wavelengths than do oxadiazoles **2** and **3** (Table 2), their luminescence spectra show only one emission band whose maximum (λ_{max}^{fl} = 421–430 nm) occupies an intermediate position between the emission maxima of benzoid and quinoid structures **I** and **V** due to the presence of ligand–metal charge-transfer band in the absorption spectra (λ_{max} = 361–366 nm). Zinc complex **4a** (L_2Zn) is characterized by a rigid tetrahedral coordination entity which hampers nonradiative deactivation of the excited state, and it shows intense luminescence (φ = 0.115–0.334) in the violet region (λ_{max}^{fl} = 427–429 nm); therefore, it may be regarded as an efficient metal complex luminophore. The emission maximum of complex **4b** is located closely to that of **4a** (λ_{max}^{fl} = 421–430 nm), but its luminescence quantum yield is very low (φ 0= .001; Table 2) because of its paramagnetic properties. The effective magnetic moment of **4b** at 298 K is μ_{eff} = 2.23 μ_B, where μ_B is the Bohr magneton equal to 927.4009×10^{-26} J/T, and it shows a strong broadened signal in the ESR spectrum ($g_{\parallel}$ = 2.086, $g_{\perp}$ = 2.027).

In summary, we have shown that the luminescence properties of oxadiazoles **2** and **3a**–**3d** and metal complexes **4a** and **4b** strongly depend on the substituent on the phenolic oxygen atom, which actively participates in photophysical processes responsible for stabilization and deactivation of the excited states. Our results make it possible to rationalize, and in some cases predict, spectral behavior of the compounds under study and their closest analogs. Quantum chemical calculations have revealed two stable conformations (**I** and **II**) of 5-(2-hydroxyphenyl)-3-methyl-1,2,4-oxadiazole with different structures of the coordination entities, which are stabilized by intramolecular hydrogen bond between the phenolic hydroxy proton and nitrogen or oxygen atom of the heterocycle. It has been found that the excited-state intramolecular proton transfer in 5-(2-hydroxyphenyl)-3-methyl-1,2,4-oxadiazole involves more stable rotamer **I**.

EXPERIMENTAL

The IR spectra were recorded from films on a Varian Excalibur 3100 FT-IR spectrometer. The ^1H and ^{13}C NMR spectra were measured at 22°C on a Bruker DPX-250 instrument (250.13 and 62.90 MHz, respectively) from solutions in $CDCl_3$ or DMSO-d_6. The mass spectra (electron impact, 70 eV) were obtained on a Finnigan MAT INCOS 50 mass spectrometer with direct sample admission into the ion source. The electronic absorption spectra were recorded on a Cary Scan 100 spectrophotometer. The luminescence spectra were measured on a Cary Eclipse spectrofluorimeter. All spectral measurements were made at room temperature. The fluorescence quantum yields were determined relative to a solution of anthracene in acetonitrile using the formula $\varphi = \varphi_0 I D_0/I_0 D n^2/n_0^2$, where φ and φ_0 are the fluorescence quantum yields of a compound under study and anthracene in acetonitrile, I and I_0 are the integral intensity of the fluorescence spectra, D and D_0 are the optical densities at the excitation wavelength, and n and n_0 are the refractive indices of the solutions, respectively. Quadratic corrections for the difference in the refractive indices

of acetonitrile and substrate solutions were included into that formula [11, 21]. The luminescence quantum yields were determined for dilute solutions with an optical density of 0.10–0.12 at the excitation wavelength. The solvents used (isooctane, toluene, methanol, acetonitrile, DMSO) were purified and dried according to standard procedures [22].

Quantum chemical calculations in terms of the density functional theory were performed using the B3LYP three-parameter functional and 6-311++G(*d*,*p*) split-valence basis set [23] (Gaussian-03). Stationary points on the potential energy surface were localized by calculating the corresponding Hessian matrices. Charges on atoms were calculated by the natural bond orbital (NBO) method.

2-(3-Methyl-1,2,4-oxadiazol-5-yl)phenol (2) was synthesized by reaction of 2-methyl-4-oxo-1,3-benzoxazinium perchlorate (**1**) with hydroxylamine according to the procedure described in [24]. Yield 67%, colorless crystals, mp 77–79°C; published data [24]: mp 76–77°C. IR spectrum, ν, cm^{-1}: 644, 657, 708, 745, 833, 1167, 1229, 1240, 1255, 1316, 1350, 1393, 1427, 1475; 1487 (C–N); 1512; 1533, 1556 (C=C); 1590, 1616 (C=N); 3179 br (OH). ^{1}H NMR spectrum ($CDCl_3$), δ, ppm: 2.51 s (3H, CH_3), 6.09–7.06 m (2H, 3′-H, 5′-H), 7.48 d.d (1H, 4′-H, ^3J = 7.5, 7.6 Hz), 7.94 d (1H, 6′-H, ^3J = 7.5 Hz), 10.47 s (1H, OH). ^{13}C NMR spectrum ($CDCl_3$), δ_C, ppm: 25.96 (CH_3), 114.10 ($C^{1'}$), 118.68 ($C^{3'}$), 119.73 ($C^{5'}$), 127.84 ($C^{4'}$), 136.01 ($C^{6'}$), 161.26 ($C^{2'}$), 168.31 (C^5), 173.80 (C^3). Mass spectrum, *m*/*z* (I_{rel}, %): 32 (45), 39 (34), 43 (12), 51 (15), 58 (17) $[CH_3C{=}NOH]^+$, 63 (48), 66 (35), 65 (34), 77 (45) $[C_6H_5]^+$, 78 (10), 82 (9), 91 (25) $[C_7H_7]^+$, 92 (98) $[C_6H_4O]^+$, 93 (22) $[C_6H_4OH]^+$, 105 (68) $[C_7H_5O]^+$, 106 (15), 119 (100) $[2\text{-}HOC_6H_4CN]^+$, 120 (87) $[2\text{-}HOC_6H_4C{=}NH]^+$, 121 (53) $[2\text{-}HOC_6H_4CO]^+$, 137 (55), 138 (12), 148 (7) $[M - CO]^+$, 161 (9) $[M - CH_3]^+$, 176 (86) $[M]^+$, 177 (25) $[M + H]^+$. *M* 176.

5-(2-Methoxyphenyl)-3-methyl-1,2,4-oxadiazole (3a) was synthesized as described in [24]. Yield 65%, colorless crystals, mp 67–68°C; published data [24]: mp 68–69°C. IR spectrum, ν, cm^{-1}: 710, 748, 1016, 1049, 1074, 1145, 1258, 1280, 1299, 1307, 1336, 1390, 1430, 1463; 1492 (C–N); 1531, 1563 (C=C); 1583, 1610 (C=N). ^{1}H NMR spectrum ($CDCl_3$), δ, ppm: 2.43 s (3H, CH_3), 3.92 s (3H, OCH_3), 6.94–7.07 m (2H, 3′-H, 5′-H), 7.47 d.d (1H, 4′-H, ^3J = 7.5, 7.6 Hz), 7.96 d (1H, 6′-H, ^3J = 7.5 Hz). ^{13}C NMR spectrum ($CDCl_3$), δ_C, ppm: 12.14 (CH_3), 56.46 (OCH_3), 112.47 ($C^{3'}$), 113.78 ($C^{1'}$), 121.12 ($C^{5'}$), 131.75 ($C^{4'}$), 134.36 ($C^{6'}$), 158.74 ($C^{2'}$), 167.64 (C^3), 174.88 (C^5). Mass spectrum, *m*/*z* (I_{rel}, %): 32 (30), 39 (28), 43 (12), 50 (30), 51 (33), 63 (41), 64 (37), 77 (42) $[C_6H_5]^+$, 78 (17), 89 (10), 90 (27), 91 (30) $[C_7H_7]^+$, 92 (32) $[C_6H_4O]^+$, 93 (15) $[C_6H_4OH]^+$, 103 (30), 104 (80) $[C_7H_4O]^+$, 105 (100) $[C_7H_5O]^+$, 107 (8) $[CH_3OC_6H_4]^+$, 119 (33) $[CH_3OC_7H_4]^+$, 122 (7), 123 (8), 133 (37) $[2\text{-}CH_3OC_6H_4CN]^+$, 134 (38) $[2\text{-}CH_3OC_6H_4C{=}NH]^+$, 135 (8) $[2\text{-}CH_3OC_6H_4CO]^+$, 148 (16) $[M - CH_3C{=}NH]^+$, 160 (9) $[M - NO]^+$, 161 (17) $[M - CHO]^+$, 173 (7) $[M - OH]^+$, 189 (14) $[M - H]^+$, 190 (23) $[M]^+$. *M* 190.

2-(3-Methyl-1,2,4-oxadiazol-5-yl)phenyl acetate (3b) was synthesized as described in [24]. Yield 54%, colorless crystals, mp 62–63°C; published data [24]: mp 61–62°C. IR spectrum, ν, cm^{-1}: 704, 720, 749, 770, 824, 869, 907, 1010, 1033, 1045, 1077, 1191, 1220, 1338, 1371, 1394, 1440; 1485 (C–N); 1528, 1567 (C=C); 1588, 1614 (C=N); 1756 (C=O). ^{1}H NMR spectrum ($CDCl_3$), δ, ppm: 2.43 s (3H, CH_3), 2.47 s (3H, CH_3CO), 7.24 d (1H, 3′-H, ^3J = 7.5 Hz), 7.43 d.d (1H, 5′-H, ^3J = 7.5, 7.6 Hz), 7.63 d.d (1H, 4′-H, ^3J = 7.5, 7.6 Hz), 8.19 d (1H, 6′-H, ^3J = 7.5 Hz). ^{13}C NMR spectrum ($CDCl_3$), δ_C, ppm: 12.09 (CH_3), 21.53 (**C**H_3CO), 118.25 ($C^{1'}$), 124.62 ($C^{3'}$), 127.03 ($C^{5'}$), 130.93 ($C^{4'}$), 134.19 ($C^{6'}$), 149.64 ($C^{2'}$), 167.93 (C^3), 170.09 (C=O), 173.18 (C^5). Mass spectrum, *m*/*z* (I_{rel}, %): 32 (15), 39 (11), 43 (100) $[CH_3CO]^+$, 50 (14), 58 (9) $[CH_3C{=}NOH]^+$, 63 (10), 64 (8), 65 (6), 77 (8) $[C_6H_5]^+$, 79 (5), 83 (7), 91 (14) $[C_7H_7]^+$, 92 (22) $[C_6H_4O]^+$, 93 (9) $[C_6H_4OH]^+$, 102 (4), 105 (8) $[C_7H_5O]^+$, 109 (5), 117 (3), 119 (30) $[2\text{-}HOC_6H_4CN]^+$, 120 (34) $[2\text{-}HOC_6H_4C{=}NH]^+$, 121 (22) $[2\text{-}HOC_6H_4CO]^+$, 130 (5), 137 (3), 147 (6) $[M - CH_3CO - CO]^+$, 155 (4), 169 (3) $[M - CH_3CH{=}NH]^+$, 176 (85) $[M + H - CH_3CO]^+$, 218 (5) $[M]^+$. *M* 218.

2-(3-Methyl-1,2,4-oxadiazol-5-yl)phenyl benzoate (3c). Benzoyl chloride, 0.47 mL (2 mmol), was added to a suspension of 0.35 g (2 mmol) of oxadiazole **2** in 0.5 mL of anhydrous pyridine. The mixture was refluxed until it became homogeneous, left to stand for 24 h at room temperature, and diluted with 50 mL of water. The precipitate was filtered off, washed with water (3×30 mL), dried in air, and recrystallized from propan-2-ol. Yield 51%, colorless crystals, mp 101–103°C. IR spectrum, ν, cm^{-1}: 703, 746, 780, 1024, 1061, 1078, 1175, 1201, 1254, 1338, 1390, 1439, 1451; 1486 (C–N); 1520, 1558 (C=C); 1584, 1611 (C=N); 1732 (C=O). ^{1}H NMR spectrum ($CDCl_3$), δ, ppm: 2.31 s (3H, CH_3), 7.34–7.58 m (4H, H_{arom}), 7.59–7.71 m (2H, H_{arom}), 8.18–8.29 m (3H, H_{arom}). ^{13}C NMR

spectrum ($CDCl_3$), δ_C, ppm: 11.94 (CH_3), 118.43 ($C^{1'}$), 124.77 ($C^{3'}$), 127.01 ($C^{5'}$), 128.97 (2C, C_6H_5), 129.88 (C_{quat}), 130.85 (2C, C_6H_5), 131.00 (C_6H_5), 131.10 ($C^{4'}$), 134.11 ($C^{6'}$), 149.90 ($C^{2'}$), 165.72 (C=O), 167.85 (C^3), 173.38 (C^5). Mass spectrum, *m*/*z* (I_{rel}, %): 32 (7), 39 (4), 43 (5), 50 (6), 51 (18), 63 (7), 64 (5), 77 (68) $[C_6H_5]^+$, 83 (4), 91 (6) $[C_7H_7]^+$, 92 (8) $[C_6H_4O]^+$, 93 (9) $[C_6H_4OH]^+$, 105 (100) $[C_6H_5CO]^+$, 106 (15), 119 (5) $[2\text{-}HOC_6H_4CN]^+$, 120 (3) $[2\text{-}HOC_6H_4C{=}NH]^+$, 121 (2) $[2\text{-}HOC_6H_4CO]^+$, 130 (2), 139 (2), 147 (3), 152 (2), 175 (5) $[M - C_6H_5CO]^+$, 209 (5), 218 (4), 236 (3) $[M - N_2O]^+$, 254 (4), 280 (15) $[M]^+$. Found, %: C 68.40; H 4.30; N 9.80. $C_{16}H_{12}N_2O_3$. Calculated, %: C 68.57; H 4.32; N 9.99. *M* 280.

2-(3-Methyl-1,2,4-oxadiazol-5-yl)phenyl 4-methylbenzenesulfonate (3g). Oxadiazole **2**, 0.34 g (2 mmol), was dissolved in 10 mL of methyl ethyl ketone, 5.52 g (8 mmol) of freshly calcined potassium carbonate and 0.37 g (2 mmol) of *p*-toluenesulfonyl chloride were added, and the mixture was refluxed for 3 h and diluted with 30 mL of ice water. The precipitate was filtered off, washed with water (3×30 mL), dried in air, and recrystallized from propan-2-ol. Yield 0.46 g (47%), colorless crystals, mp 87–89°C. IR spectrum, ν, cm^{-1}: 699, 734, 767, 783, 802, 823, 861, 1043, 1088; 1171 (SO_2); 1198, 1298, 1312, 1343; 1374 (SO_2); 1448, 1467; 1495 (C–N); 1556, 1588 (C=C); 1595, 1615 (C=N). ^{1}H NMR spectrum ($CDCl_3$), δ, ppm: 2.38 s (3H, CH_3), 2.40 s (3H, C**H**$_3$C$_6$H$_4$), 7.23 d (2H, *o*-H, ^3J = 7.5 Hz) , 7.41 d.d (1H, 5′-H, ^3J = 7.5, 7.6 Hz), 7.45 d (1H, 3′-H, ^3J = 7.6 Hz), 7.57 d.d (1H, 4′-H, ^3J = 7.5, 7.6 Hz), 7.65 d (2H, *m*-H, ^3J = 7.5 Hz), 7.96 d (1H, 6′-H, ^3J = 7.5 Hz). ^{13}C NMR spectrum ($CDCl_3$), δ_C, ppm: 11.97 (CH_3), 22.11 (**C**$H_3C_6H_4$), 119.29 ($C^{1'}$), 125.10 ($C^{3'}$), 127.95 ($C^{5'}$), 129.01 and 129.98 (C^o, C^m), 131.52 ($C^{4'}$), 132.36 (C^i), 134.05 ($C^{6'}$), 146.07 (C^p), 147.59 ($C^{2'}$), 167.69 (C^3), 172.99 (C^5). Mass spectrum, *m*/*z* (I_{rel}, %): 32 (5), 39 (8), 43 (6), 50 (7), 51 (6), 63 (10), 64 (9), 65 (25), 76 (7), 77 (8) $[C_6H_5]^+$, 89 (5), 91 (100) $[C_7H_7]^+$, 92 (18) $[C_6H_4O]^+$, 102 (4), 105 (8) $[C_7H_5O]^+$, 119 (4) $[2\text{-}HOC_6H_4CN]^+$, 120 (4) $[2\text{-}HOC_6H_4C{=}NH]^+$, 121 (3) $[2\text{-}HOC_6H_4CO]^+$, 132 (2), 139 (3), 147 (4), 155 (53) $[CH_3C_6H_4SO_2]^+$, 164 (3), 176 (8) $[M + H - CH_3C_6H_4SO_2]^+$, 182 (4), 208 (5), 245 (5), 266 (48) $[M - SO_2]^+$, 330 (6) $[M]^+$. Found, %: C 58.30; H 4.30; N 8.60; S 9.60. $C_{16}H_{14}N_2O_4S$. Calculated, %: C 58.17; H 4.27; N 8.48; S 9.71. *M* 330.

Bis[(3-methyl-1,2,4-oxadiazol-5-yl)phenolato]-zinc(II) (4a) was synthesized as described in [25]. Yield 55%, colorless crystals, mp 267–269°C; published data [25]: mp 266°C. IR spectrum, ν, cm^{-1}: 715, 752, 959, 1044, 1084, 1138, 1164, 1245, 1320, 1352, 1393, 1435; 1477 (C–N); 1530, 1552 (C=C); 1573, 1606 (C=N). ^{1}H NMR spectrum (DMSO-d_6), δ, ppm: 2.63 s (3H, CH_3), 6.51 d.d (1H, 5′-H, ^3J = 7.5, 7.6 Hz), 6.72 d (1H, 3′-H, ^3J = 7.6 Hz), 7.26 d.d (1H, 5′-H, ^3J = 7.5, 7.6 Hz), 7.73 d (1H, 6′-H, ^3J = 7.5 Hz). Mass spectrum, *m*/*z* (I_{rel}, %): 32 (15), 39 (27), 41 (33), 43 (9), 51 (18), 53 (19), 58 (14) $[CH_3C{=}NOH]^+$, 64 (31), 66 (17), 77 (12) $[C_6H_5]^+$, 78 (9), 91 (29) $[C_7H_7]^+$, 92 (37) $[C_6H_4O]^+$, 93 (6) $[C_6H_4OH]^+$, 94 (78), 105 (8) $[C_7H_5O]^+$, 119 (44) $[2\text{-}HOC_6H_4CN]^+$, 120 (52) $[2\text{-}HOC_6H_4C{=}NH]^+$, 121 (28) $[2\text{-}HOC_6H_4CO]^+$, 143 (11), 155 (4), 176 (100) $[LH]^+$, 183 (31), 185 (7), 242 (63) $[L_2{}^{64}Zn - L]^+$, 244 (35) $[L_2{}^{66}Zn - L]^+$, 291 (3), 327 (5), 363 (6), 379 (4), 400 (3), 414 (22) $[L_2{}^{64}Zn]^+$, 416 (12) $[L_2{}^{66}Zn]^+$. *M* 415.

Bis[(3-methyl-1,2,4-oxadiazol-5-yl)phenolato]-copper(II) (4b) was synthesized as described in [25]. Yield 59%, light brown crystals, mp 230–232°C; published data [25]: mp 228°C. IR spectrum, ν, cm^{-1}: 715, 748, 772, 854, 959, 1051, 1085, 1141, 1167, 1252, 1306, 1336, 1394, 1429; 1471 (C–N); 1533, 1548 (C=C); 1572, 1607 (C=N). Mass spectrum, *m*/*z* (I_{rel}, %): 32 (18), 39 (35), 40 (12), 43 (8), 50 (14), 51 (20), 52 (15), 53 (13), 58 (17) $[CH_3C{=}NOH]^+$, 63 (72), 64 (42), 65 (32), 76 (9), 77 (8) $[C_6H_5]^+$, 78 (10), 91 (31) $[C_7H_7]^+$, 92 (82) $[C_6H_4O]^+$, 93 (13) $[C_6H_4OH]^+$, 104 (17), 105 (8) $[C_7H_5O]^+$, 106 (9), 119 (64) $[2\text{-}HOC_6H_4CN]^+$, 120 (83) $[2\text{-}HOC_6H_4C{=}NH]^+$, 121 (67) $[2\text{-}HOC_6H_4CO]^+$, 129 (4), 139 (4), 141 (11), 155 (4), 176 (100) $[LH]^+$, 181 (19), 183 (40), 185 (15), 238 (65) $[L_2{}^{63}Cu - L]^+$, 239 (8), 240 (29) $[L_2{}^{65}Cu - L]^+$, 254 (3), 272 (2), 291 (3), 300 (3), 327 (3), 342 (2), 363 (4), 379 (3), 400 (2), 413 (16) $[L_2{}^{63}Cu]^+$, 414 (2), 415 (7) $[L_2{}^{65}Cu]^+$. *M* 414.

ACKNOWLEDGMENTS

This study was performed under financial support by the Ministry of Education and Science of the Russian Federation in the framework of state assignment (project no. 4.129.2014/K).

REFERENCES

1. Jiang, P. and Guo, Z., *Coord. Chem. Rev*., 2004, vol. 248, p. 205. DOI: 10.1016/j.cct.2003.10.013.
2. Mikhailov, I.E., Kolodina, A.A., Dushenko, G.A., Artyushkina, Yu.M., Tkachev, V.V., Aldoshin, S.M., Sayapin, Yu.A., and Minkin, V.I., *Chem. Heterocycl. Compd*., 2014, vol. 50, no. 6, p. 828. DOI: 10.1007/s10593-014-1537-9.

3. Mikhailov, I.E., Dushenko, G.A., Starikov, D.A., Mikhailova, O.I., and Minkin, V.I., *Vestn. Yuzhn. Nauch. Tsentra*, 2010, vol. 6, no. 4, p. 32.
4. Mikhailov, I.E., Kolodina, A.A., Artyushkina, Yu.M., Dushenko, G.A., Sayapin, Yu.A., and Minkin, V.I., *Russ. J. Org. Chem*., 2015, vol. 51, no. 4, p. 595. DOI: 10.1134/S1070428015040235.
5. Wang, G., Zhang, Y.G., Cheng, Y.X., Ma, D.G., Wang, L.X., Jing, X.B., and Wang, F.S., *Synth. Met*., 2003, vol. 137, nos. 1–3, p. 1119. DOI: 10.1016/S0379-6779(02)01106-2.
6. Pace, A. and Pierro, P., *Org. Biomol. Chem*., 2009, vol. 7, no. 6, p. 4337. DOI: 10.1039/b908937c.
7. Ryabukhin, Yu.I., Mezheritskii, V.V., and Dorofeenko, G.N., *Zh. Obshch. Khim*., 1974, vol. 44, no. 12, p. 2792.
8. Da Silva, A.S., De Silva, M.A.A., Carvalho, C.E.M., Antunes, O.A.C., Herrera, J.O.M., Brinn, I.M., and Mangrich, A.S., *Inorg. Chim. Acta*, 1999, vol. 292, p. 1. DOI: 10.1016/S0020-1693(99)00108-5.
9. Vikrishchuk, A.D., Popov, L.D., Vikrishchuk, N.I., Morozov, P.G., and Mikhailov, I.E., *Russ. J. Gen. Chem*., 2011, vol. 81, no. 1, p. 132. DOI: 10.1134/S107036321101021X.
10. Beldovskaya, A.D., Dushenko, G.A., Vikrishchuk, N.I., Popov, L.D., Revinskii, Yu.V., and Mikhailov, I.E., *Russ. J. Gen. Chem*., 2013, vol. 83, no. 11, p. 2075. DOI: 10.1134/S1070363213110200.
11. Doroshenko, A.O., Posokhov, E.A., Verezubova, A.A., and Ptyagina, L.M., *J. Phys. Org. Chem*., 2000, vol. 13, no. 5, p. 253. DOI: 10.1002/1099-1395(200005).
12. Beldovskaya, A.D., Dushenko, G.A., Vikrishchuk, N.I., Popov, L.D., Revinskii, Yu.V., Mikhailov, I.E., and Minkin, V.I., *Russ. J. Gen. Chem*., 2014, vol. 84, no. 1, p. 171. DOI: 10.1134/S1070363214010290.
13. Dushenko, G.A., Vikrishchuk, A.D., Mikhailov, I.E., and Vikrishchuk, N.I., *Vestn. Yuzhn. Nauch. Tsentra*, 2013, vol. 9, no. 1, p. 37.
14. Serdyuk, O.V., Evseenko, I.V., Dushenko, G.A., Revinskii, Yu.V., and Mikhailov, I.E., *Russ. J. Org. Chem*., 2012, vol. 48, no. 1, p. 78. DOI: 10.1134/S1070428012010113.
15. Mikhailov, I.E., Svetlichnyi, D.A., Burov, O.N., Revinskii, Yu.V., Dushenko, G.A., and Minkin, V.I., *Russ. J. Gen. Chem*., 2015, vol. 85, no. 5, p. 1074. DOI: 10.1134/S1070363215050126.
16. Beldovskaya, A.D., Dushenko, G.A., Vikrishchuk, N.I., Popov, L.D., Revinskii, Yu.V., Mikhailov, I.E., and Minkin, V.I., *Russ. J. Org. Chem*., 2013, vol. 49, no. 12, p. 1861. DOI: 10.1134/S1070428013120312.
17. Mikhailov, I.E., Popov, L.D., Vikrishchuk, N.I., Beldovskaya, A.D., Revinskii, Yu.V., Dushenko, G.A., and Minkin, V.I., *Russ. J. Gen. Chem*., 2015, vol. 85, no. 1, p. 203. DOI: 10.1134/S1070363215010363.
18. Zhang, H., Han, Li.-F., Zachariasse, K.A., and Jiang, Y.-B., *Org. Lett*., 2005, vol. 7, no. 19, p. 4217. DOI: 10.1021/ol051614h.
19. Krasovitskii, B.M. and Bolotin, B.M., *Organicheskie lyuminofory* (Organic Luminophores), Moscow: Khimiya. 1984, p. 11.
20. Zhang, H., Wang, Q.-Li., and Jiang, Y.-B., *Tetrahedron Lett*., 2007, vol. 48, no. 23, p. 3959. DOI: 10.1016/j.tetlet.2007.04.045.
21. Kotelevskiy, S.I., *J. Lumin*., 1998, vol. 79, no. 3, p. 211.
22. Weissberger, A., Proskauer, E.S., Riddick, J.A., and Toops, E.E., Jr., *Organic Solvents: Physical Properties and Methods of Purification*, New York: Intersci., 1955, 2nd ed.
23. Foresman, J.B. and Frisch, E., *Exploring Chemistry with Electronic Structure Methods*, Pittsburg: Gaussian, 1996.
24. Ryabukhin, Yu.I., Eliseeva, A.Yu., Suzdalev, K.F., Bulgarevich, S.B., Movshovich, D.Ya., Knyazev, A.P., Terent'ev, P.V., and Yusman, T.A., *Chem. Heterocycl. Compd*., 1992, vol. 28, no. 4, p. 454.
25. Ryabukhina, O.I., Yusman, T.A., Ryabukhin, Yu.I., Garnovskii, A.D., and Dorofeenko, G.N., *Koord. Khim*., 1980, vol. 6, no. 8, p. 1186.